Type III Collagen Modulates Fracture Callus Bone Formation and Early Remodeling

Emily L. Miedel,[1,*] Becky K. Brisson,[2,*] Todd Hamilton,[2] Hadley Gleason,[2] Gary P. Swain,[2] Luke Lopas,[3] Derek Dopkin,[3,4,5] Joseph E. Perosky,[6] Kenneth M. Kozloff,[6,7] Kurt D. Hankenson,[3,4,5] Susan W. Volk[2]

[1]Department of Pathobiology, School of Veterinary Medicine, University of Pennsylvania, Philadelphia, Pennsylvania, [2]Department of Clinical Studies-Philadelphia, School of Veterinary Medicine, University of Pennsylvania, Philadelphia, Pennsylvania, [3]Department of Orthopaedic Surgery, Perelman School of Medicine, University of Pennsylvania, Philadelphia, Pennsylvania, [4]Department of Small Animal Clinical Sciences, Michigan State University, East Lansing, Michigan, [5]Department of Physiology, Michigan State University, East Lansing, Michigan, [6]Orthopaedic Research Laboratories, Department of Orthopaedic Surgery, University of Michigan, Ann Arbor, Michigan, [7]Department of Biomedical Engineering, University of Michigan, Ann Arbor, Michigan

Received 1 August 2014; accepted 19 January 2015
Published online 8 March 2015 in Wiley Online Library (wileyonlinelibrary.com). DOI 10.1002/jor.22838

ABSTRACT: Type III collagen (Col3) has been proposed to play a key role in tissue repair based upon its temporospatial expression during the healing process of many tissues, including bone. Given our previous finding that Col3 regulates the quality of cutaneous repair, as well as our recent data supporting its role in regulating osteoblast differentiation and trabecular bone quantity, we hypothesized that mice with diminished Col3 expression would exhibit altered long-bone fracture healing. To determine the role of Col3 in bone repair, young adult wild-type (Col3+/+) and haploinsufficent (Col3+/−) mice underwent bilateral tibial fractures. Healing was assessed 7, 14, 21, and 28 days following fracture utilizing microcomputed tomography (microCT), immunohistochemistry, and histomorphometry. MicroCT analysis revealed a small but significant increase in bone volume fraction in Col3+/− mice at day 21. However, histological analysis revealed that Col3+/− mice have less bone within the callus at days 21 and 28, which is consistent with the established role for Col3 in osteogenesis. Finally, a reduction in fracture callus osteoclastic activity in Col3+/− mice suggests Col3 also modulates callus remodeling. Although Col3 haploinsufficiency affected biological aspects of bone repair, it did not affect the regain of mechanical function in the young mice that were evaluated in this study. These findings provide evidence for a modulatory role for Col3 in fracture repair and support further investigations into its role in impaired bone healing. © 2015 Orthopaedic Research Society. Published by Wiley Periodicals, Inc. J Orthop Res 33:675–684, 2015.

Keywords: type III collagen; fracture; extracellular matrix

Regenerative medicine seeks to restore function to damaged tissues. Approximately 1.5 million bone graft procedures are performed in the United States each year in an attempt to improve problematic skeletal healing, with an overall annual global economic burden valued at over $1 billion.[1,2] Despite the use of such procedures, as well as advances in synthetic biomaterials and biological therapeutics, fracture complications in trauma patients remain a formidable clinical problem. The resulting morbidity and healthcare expenditure underscores the need to develop novel treatments. Research that elucidates critical biological components of adjunctive therapies, including "smarter" biomaterials, is clearly needed.

Type III collagen (Col3) is a homotrimeric fibril-forming collagen found in many connective tissues. Col3 expression is increased during development as well as early in the healing process of a variety of tissues such as bone, tendon, ligament, and skin.[3–5] Fracture callus has been shown to contain considerable amounts of Col3, which is later replaced by type 1 collagen (Col1).[6–8] However, the role of Col3 in tissue repair has remained enigmatic. Until recently, the only known role of Col3 in tissue homeostasis involved regulation of type I collagen (Col1) fibrillogenesis.[9] Our laboratory has recently shown that Col3 plays an important role in cutaneous wound repair, that is, distinct from type I collagen in its ability to promote a regenerative response and limit scar formation.[10] Specifically, Col3 deficiency results in increased scar deposition by promoting differentiation of myofibroblasts, the key cells that influence pathologic scarring. Furthermore, we have recently shown that Col3 regulates osteoblastogenesis and the quantity of trabecular bone.[11] In addition to its expression in the early fracture callus,[4,12] several lines of evidence support a role for Col3 in repair and maintenance of bone, including its requirement for growth acceleration of osteoblasts,[13] its potential role in preserving osteogenic potential of mesenchymal stem cells,[14] and its ability to increase angiogenesis.[15]

A critical role for Col3 in both maintenance and repair of tissues and organs, including the skeleton, is equally apparent in human clinical medicine. Patients with vascular Ehlers–Danlos syndrome (EDS), who have mutations or deficiency in Col3, have structural failure and poor repair of cardiovascular, gastrointestinal, and urogenital tissues.[16,17] Although death in vascular EDS patients is most often associated with catastrophic failure of these soft tissue structures, patients also have been reported to display numerous skeletal abnormalities including a distinctive facial appearance, spinal deformity, scoliosis, club foot, temporal mandibular disorder, and osteoporosis.[18–20] Although poor repair of

Conflicts of interest: None.
*These authors contributed equally.
Grant sponsor: National Institutes of Health (NIAMS) supported Penn Center for Musculoskeletal Disorders (AR050950) (SWV); Grant sponsor: National Institutes of Health (SWV); Grant number: K08AR053945.
Correspondence to: Susan W. Volk (T: +1-215-898-0635; F: +1-215-746-2295; E-mail: swvolk@vet.upenn.edu)

affected soft tissue organs in vascular EDS patients is well documented, it is unknown if diminished Col3 has significant effects on repair of the skeletal system, including long bone fracture. Notably, Col3 levels decline with age, and low levels are also associated with diabetes, smoking, certain medications (i.e. steroids), and the post-menopausal state[21–27]—all risk factors for poor bone healing.

Given the data supporting a critical role for Col3 in tissue repair and regeneration and its role in skeletal development and maintenance, we investigated the hypothesis that diminished Col3 would negatively impact fracture repair through its effects on progenitor and reparative cell function and recruitment to sites of injury. Because of the potential clinical relevance of diminished rather than absent Col3, the poor survival of Col3-null mice (<5% beyond weaning[9,11]), and the current lack of availability of conditional Col3 transgenic mice, fracture repair was assessed in Col3 wild-type, and haploinsufficient littermates. Previously, Col3 haploinsufficient mice were found to express half the amount of Col3 in tissues compared to wild-type littermates.[9,28,29] Our recent work confirmed that Col3 expression in long bones of Col3+/− mice is approximately half of that seen in Col3+/+ mice.[11] In this study, using a bilateral closed, transverse tibial fracture mouse model, we show that diminished Col3 leads to decreased bone formation and alterations in remodeling during fracture healing. These findings suggest that Col3 may play an important role during fracture healing and support further studies to determine the impact of a complete absence of Col3 on fracture repair and under circumstances in which fracture repair would be delayed such as in aged individuals or those with ischemic injury.

METHODS

Experimental Design

Animal utilization and care was approved by the Institutional Animal Care and Use Committee (IACUC) of the University of Pennsylvania and followed guidelines set forth in the National Institutes of Health Guide for the Care and Use of Laboratory Animals. To determine expression of Col3 temporally during fracture repair in this tibial fracture model, mRNA that had been characterized previously for markers of bone healing[30] was used to quantify gene expression of Col3 and Col1 at 2, 5, 10, and 20 days post fracture (dpf; $n = 4$–5) using quantitative real-time polymerase chain reaction (QPCR). Then to investigate the effect of diminished Col3 on the process of fracture repair, bilateral tibial fractures were performed on 12–16 week old female Col3 wild-type (+/+) mice and Col3 deficient (+/−) littermates. Specimens were harvested at 7, 14, 21, and 28 days post-fracture (dpf). MicroCT analysis using a vivaCT 40 MicroCT system (Scanco Medical, Switzerland) was performed to evaluate bone and callus volume. After microCT, tibiae were prepared for histology and immunohistochemistry/fluorescence. Specifically, immune-localization for Col3, Safranin-O staining to analyze cartilage, immunohistochemistry for proliferating cell nuclear antigen (PCNA) to identify cellular proliferation and tartrate resistant acid phosphatase (TRAP) staining to assess osteoclastic activity were performed using histologic sections of fractures. Finally, a comparison of fracture biomechanics between the two genotypes was performed by torsion testing.

QPCR

Temporal expression of Col3 in fracture repair was assessed using previously generated cDNA isolated from fractures spanning the time frame examined in this study.[31] Briefly, gene expression was quantified from cDNA of mRNA purified from day 2, 5, 10, and 20 fracture calluses ($n = 4$ or 5 per time point) using a 7500 Fast Real-Time PCR system (Applied Biosystems, Life Technologies, Grand Island, NY) from a total of 10 μl of Master Mix per well, which included 1× Fast SYBR Green (Applied Biosystems), 0.5 μl of cDNA, and previously described forward and reverse primers (0.45 μM) for Col1, Col3, and GAPDH.[11] For each gene of interest, samples were run in triplicate and results analyzed as previously described.

Production and Genotyping of Col3-Deficient Mice

All mice for this study were generated in a colony established at the University of Pennsylvania from breeder pairs of Col3A1 heterozygous (Col3+/–) mice originally purchased from Jackson Laboratories (Bar Harbor, ME). These mice had been generated by homologous recombination by replacement of the promoter region and first exon of the Col3 gene with a 1.8-kb PGKneo cassette.[9] Animals were genotyped for Col3 by PCR analysis of DNA extracted from tail biopsies as described previously.[11] At the time of genotyping, mice were microchipped for identification (Allflex FDX-B transponders; Allflex USA, Inc., Dallas, TX). All mice were identified based upon the last four digits of the implanted microchip to maintain blinding of genotype during analysis, as previously described.[10]

Tibial Fracture Procedure

Closed, transverse, mid-diaphyseal bilateral tibial fractures were created similar to previously published methods.[32] Briefly, under isoflurane anesthesia, a small incision was made medial to the tibial tuberosity. The bone cortex was punctured using a 26-gauge needle, and a 0.009-inch sterile diameter rod was inserted through the length of the intramedullary canal. The incision was closed with surgical glue (GLUture; Abbott Laboratories, Abbott Park, IL). Fractures were created using a custom made three-point bending apparatus. Buprenorphine (0.05 mg/kg) was administered subcutaneously prior to and twice daily for 3 days after surgery for analgesia.

Tissue Harvest and Preparation

All mice were euthanized via CO_2 inhalation. Fractured tibiae were carefully dissected and fixed in 4% paraformaldehyde (PFA) at 4°C for 24–48 h. The intramedullary pins were then removed and tibiae were transferred to 70% ethanol until further processing for microCT. After microCT, the legs were decalcified in 15% formic acid for 14 h, then were dehydrated in ethanol and embedded in paraffin as previously described.[30] Sagittal sections (8 μm) through the block were prepared for histology and immunofluorescence (IF) and immunohistochemistry (IHC).

IF and IHC

For Col3 immunolocalization studies, sections of fractured tibias (7, 14, and 28 dpf) were mounted on positively charged slides (Fisher Scientific, Pittsburgh, PA) that were treated

with VectaBond (Vector Laboratories Inc., Burlingame, CA) to ensure bone adherence to the slides. After heating at 60°C overnight, sections were deparaffinized in xylene and rehydrated through ethanols to water. Antigen retrieval was carried out using pepsin (Worthington Biomedical Corporation, Lakewood, NJ, 1 mg/ml, 37°C, 1 h, 0.01 N HCl).[33] Slides were blocked in 5% BSA and exposed to a Col3 primary antibody (ab7778; Abcam, Cambridge, MA) for 72 h at 4°C. After incubation with the primary antibody, slides were washed and exposed to secondary antibody Alexa Fluor 488 goat anti-rabbit F(ab')$_2$ fragment (Invitrogen, Grand Island, NY) at 1:500 for 30 min at 37°C, washed and stained with 4,6-diamidino-2-phenylindole (DAPI; Vector Laboratories Inc.). Sections incubated without primary antibody served as negative controls. Qualitative 100× and 200× images were taken on a Leica DM RBE fluorescent microscope equipped with a Q-Imaging Retiga 2000 CCD camera (QImaging Surry, BC, Canada) controlled by iVision software (Biovision, Exton, PA).

For peroxide-based immunohistochemistry, sections of the fractured tibia at 7, 14, or 21 dpf (4–5 samples per group) were deparaffinized, rehydrated and immersed in heated sodium citrate buffer. Slides were blocked and exposed to the primary antibody of PCNA (Abcam). After treatment with the primary antibody (PCNA, 1:1,000), sections underwent peroxidase blocking with 3% H_2O_2 and were then treated with biotin-conjugated secondary antibody at 1:200 (Santa Cruz Biotechnology, Santa Cruz, CA). After secondary antibody treatment, slides were incubated with streptavidin-conjugated horseradish peroxidase (HRP; Abcam) and then with 3,3′-diaminobenzidine (DAB) as the chromogen. Slides were counterstained with Gill's hematoxylin, dehydrated, mounted using Permount (Biomeda, Foster City, CA) and visualized using an Olympus BX51 light microscope and Spot RT3 camera. Negative controls were sections with no primary antibody staining. Skin sections served as positive controls.

Safranin-O Histology

Safranin-O staining was performed to determine the total cartilage area within the fracture callus. Briefly, slides of the fractured left tibia were deparaffinized, rehydrated, stained with hematoxylin, rinsed in dH_20, exposed to 0.3% Fast Green FCF, rinsed in 1% acetic acid, immersed in 0.1% Safranin-O, rinsed in dH_2O, dehydrated and mounted. These samples were used for measuring total cartilage area within the fracture callus, as described previously.[30]

Histomorphometry

As previously described,[30] Safranin-O positive area of the callus was measured at 20× magnification using MetaMorph Image Analysis software (Molecular Devices, Sunnyvale, CA). Contours of the fracture callus were manually defined and then color threshold was applied to identify areas of Safranin-O positive staining within the callus. The thresholded area was divided into total area to calculate the percentage.

For quantification of PCNA, two to three areas of undifferentiated mesenchyme adjacent to the fracture callus per sample were captured using a 40× objective (400×) and were analyzed using ImageJ software (National Institutes of Health, Bethesda, MD [http://rsb.info.nih.gov/ij/]), as previously described.[30] High resolution TIF images were imported into ImageJ, and then the Color Deconvolution plugin (http://www.dentistry.bham.ac.uk/landinig/software/cdeconv/cdeconv.html) was applied to differentiate positive (brown) from negative (blue) cells. Thresholding was applied to separate positive and negative cells into discrete images, and then the "Analyze Particles" command was executed to count the cells. The percent of positive cells was determined by comparing the number of positive cells to the total number of cells. The average between samples was taken and standard error was computed.

Assessment of Osteoclast Numbers

Osteoclasts were identified by positive staining for TRAP activity using the Acid Phosphatase, Leukocyte (TRAP) kit (Sigma, St Louis, MI), following the manufacturer's instructions. Histologic sections from PFA fixed, paraffin embedded samples (day 21 and 28) described above were utilized (Col3+/+ $n=4$ dpf 21, $n=7$ dpf 28) and Col3+/− ($n=5$ dpf 21, $n=6$ dpf 28). Paraffin was removed with xylene, and sections were rehydrated in decreasing concentrations of ethanol. For each sample, osteoclasts were counted in three non-overlapping 200× fields within the callus and the bone surface perimeter was traced and quantified using ImageJ.

Woven Bone Histology Measurements

Histologic sections were processed and stained with hematoxylin and eosin (H&E) as described.[18] (Col3+/+ mice: $n=4$ dpf 21, $n=7$ dpf 28; Col3+/− mice: $n=5$ dpf 21, $n=6$ dpf 28). One 200× brightfield image was taken for each fracture, capturing the entire callus. Using ImageJ, bone was selected based on a color threshold. The cortical bone was not included in the analysis, and the perimeter (bone surface) of the remaining woven bone was measured.

Micro-Computed Tomography

Tibiae were wrapped in 70% ethanol-soaked gauze and scanned using a vivaCT 40 MicroCT system (Scanco Medical) with an isotropic 3D voxel size of 21 μm. A semi-automated contouring method was used to determine the callus perimeter. Briefly, callus and cortical bone sections were manually identified on the first slice and then had spline interpolation between points. The points were chosen on slices no more than ten slices apart (0.105 mm). These points were manually reviewed across every slice and re-interpolation was performed if necessary. The cortical bone sections were removed from the image, and a global threshold was applied that calculated bone volume, tissue mineral density, bone mineral density, callus (tissue) volume, bone volume fraction, bone mineral content and tissue mineral content. Any comminuted fracture, or fracture not located mid-shaft, was excluded from analysis.[30]

Biomechanical Testing

A randomly assigned subset of the fractured tibiae was tested in torsion, as previously described.[34] These fractures had been fixed and stored as described above. Prior to biomechanical testing, bones were rehydrated in PBS for 3 h as previously described.[35] Whole bone specimens were potted using a low-melting temperature bismuth alloy (Cerrobend, Cerro Products, Bellefont, PA), mounted in a torsion mechanical testing system (Bose ElectroForce 3300, Bose Corporation, Eden Prairie, MN), and tested in external rotation at 0.3°/s until failure. Using a MATLAB script, raw data were filtered and stiffness, angular displacement at failure, torque at failure, and energy to failure were measured.

Statistical Analysis

Values are expressed as mean ± standard error of the mean (SEM) in the text and figures, unless otherwise stated.

Normality was determined using the Shapiro–Wilk test. Unpaired student's *t*-tests or the Wilcoxon Rank Sum test was utilized to determine statistical significance between two groups of normally distributed or non-normally distributed data, respectively. When multiple comparisons were performed, significance between groups was assessed by one way analysis of variance (ANOVA), followed by a Tukey's posthoc test, or a 2-way ANOVA followed by a Bonferroni posthoc test to determine significance between groups. Unadjusted *p*-values less than or equal to the critical level set by the posthoc test after multiple comparisons were made were considered significant. Study groups were compared utilizing SigmaPlot software (Systat Inc., Chicago, IL). *p*-values <0.05 were considered statistically significant.

RESULTS

Col3 Expression is Increased During Fracture Repair

To determine the expression pattern of Col3 during fracture repair in our closed tibial fracture model, we performed QPCR using samples that had previously been characterized for chondrogenic and osteogenic marker expression.[31] Consistent with previous reports of an increase in Col3 expression during the early repair process of a variety of tissues, including bone, an increase in Col3 was evident by day two post-fracture. Col3 expression was significantly elevated starting at day 5 ($p < 0.05$) and up to 20 days post-fracture compared to non-injured bone (Fig. 1A). Similar to previous reports, an increase in expression of type I collagen (Col1) lags behind that of Col3 with significant ($p < 0.01$) elevation over baseline levels not occurring until day 20 post-fracture.[36] To assess distribution of Col3 in the fracture callus, we performed immunoflourescent localization in day 7, 14, and 28 fractures. Consistent with previous publications examining bone Col3 expression in other species,[6–8,37–39] we found that minimal to no Col3 expression could be found in mature (uninjured) cortical bone, although Col3 expression could be detected in trabeculae and was found to be highly expressed within the periosteum (Fig. 1B). Within the early fracture callus (day 7; Fig. 1C), Col3 was found within the undifferentiated mesenchyme and to a lesser extent in the cartilage. At later stages of healing, Col3 can be visualized in the walls of newly formed vessels, as well as trabeculae (days 14 and 28; Fig. 1D and E). By comparison, Col3 expression was diminished within the cartilage where it can be visualized surrounding only a subset of chondrocytes at day 14 (Fig. 1D), similar to previous reports in the rabbit and rat.[6,7] In the newly formed bone of day 28 fractures, Col3 containing fibers were found in the immature woven bone but were absent in more mature lamellar bone, suggesting Col3 is replaced as remodeling progresses and returns to a steady state level (Fig. 1E).

Callus Cartilage Volume Is Not Significantly Affected by Col3 Levels During Fracture Healing

Since Col3 is elevated early during the fracture healing process, coincident with cartilage formation, we next investigated whether endochondral ossification was altered with Col3 deficiency. At day 14 and 21 after fracture, there was no significant difference seen in percent cartilage composition of the callus between Col3 haploinsufficient and wild-type mice (Fig. 2), although there was a trend for Col3 haploinsufficient mice to have increased cartilage at day 14 (50% increase). This could indicate a delay in endochondral ossification, or may be reflective of more cartilage forming in the callus of Col3+/− mice relative to that in wild-type mice. By day 21, calluses from both groups of mice had formed a boney union and contained little to no detectable cartilage.

MicroCT Analysis of Tibial Fracture in Young Adult Col3+/+ and Col3+/− Mice

Given our previous findings that Col3 deficiency negatively impacts osteogenesis in vitro and trabecular bone quantity in vivo, we next examined the amount of bone that forms in the callus. Surprisingly, μCT analysis showed that, overall, there were few significant differences in the bone that forms in the callus of Col3+/− and Col3+/+ mice at 14, 21, or 28 days after fracture (Fig. 3). However, bone volume fraction (bone volume/total callus volume) and bone mineral density were significantly higher in Col3+/− mice compared to Col3+/+ littermates at day 21 post-fracture (Fig. 3C and D). This finding was likely due to the smaller callus volume seen in Col3+/− mice (although not significant) at this time point (Fig. 3A), suggesting that the Col3 haploinsufficient mice exhibit altered fracture healing dynamics. By day 28, however, tissue (callus) volume was decreased in both groups with enhanced Bone Mineral Densities, consistent with callus maturation between day 21 and 28 (Fig. 3A, C, and D), suggesting remodeling at this time between both groups of mice.

The Content of Bone Within the Fracture Callus Is Significantly Reduced in Col3+/− Mice

Interestingly, histologic examination of calluses from 21-day-old fractures suggested that Col3+/− mice had a reduction in the amount of bone present within the callus compared to Col3+/+ mice. Quantitative analysis of total bone surface within the callus confirmed that Col3+/− mice had significantly less bone surface compared to wild-type mice (Fig. 4). This difference was most pronounced at day 21, but continues through day 28 fractures. It is notable that histological bone surface (Fig. 4) decreased from days 21 to 28 in both the Col3+/+ and Col3+/− mice, consistent with the decrease in bone volume observed with microCT (Fig. 3B). It should be noted that no significant differences were found in biomechanical properties between fractured tibia (day 28) of the two genotypes in torsion testing (Supplemental Table S1).

Mesenchymal Cell proliferation Within the Fracture Callus Is Not Significantly Different Between Col3+/− and Col3+/+ Mice

To further characterize whether the discrepancy in bone surface area in Col3+/− and Col3+/+ mice was the

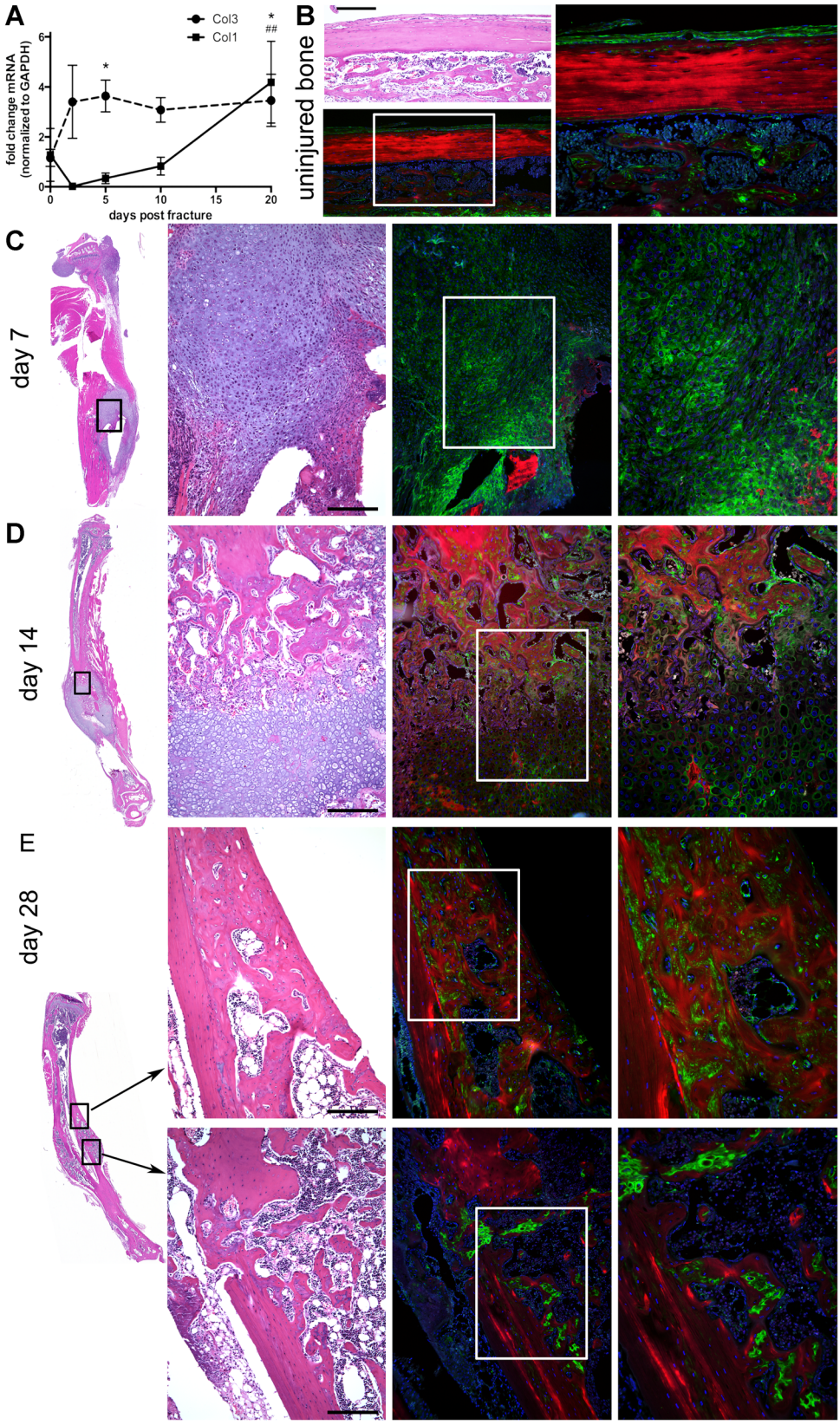

Figure 1. Col3 expression is upregulated by day 2 after fracture and remains elevated until at least day 28 after fracture. Quantitative real-time RT-PCR was performed on fractured tibia of mice on C57Bl/6 background ($n = 4$ or 5 per group) for Col1 and Col3 expression. Results are presented as the fold-change of mRNA normalized to GAPDH (mean ± SD), which was used as the endogenous control. Col3 is significantly higher than base line (0 day post fracture) at days 5 and 20 post-fracture ($^{*}p < 0.05$), while significant elevation in Col1 above base line did not occur until day 20 ($^{\#\#}p < 0.01$). (B–E) Bone H&E and Col3 immunofluorescent staining to show Col3 localization during fracture healing. Green, Col3; Red, bone autofluorescence; Blue, DAPI. Scale bars = 200 μm. (B) 10× and 20× images of uninjured bone. 20× field of view is boxed in 10× image. (C–E) Whole tibia, 10× and 20× images of day 7 (C), 14 (D), and 28 (E) post fracture callus. 10× field of view is boxed in whole tibia image, and 20× field of view is boxed in 10× image.

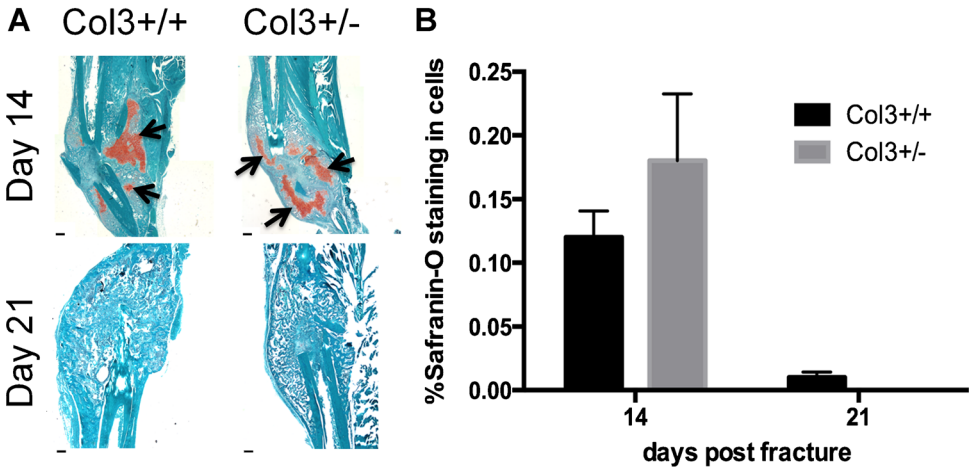

Figure 2. Histological analysis of fracture calluses does not show differences in cartilage composition during healing. (A) Safranin-O staining in tibial fractures in wildtype and Col3 haploinsufficient mice (days 14 and 21 post fracture), revealing the presence of proteoglycan (arrows). By day 21, there is little to no cartilage present in the fracture callus. Scale bar = 400 μm. (B) Quantification of percent cartilage found in fracture callus day 14 and 21 after fracture ($n = 4$ or 5).

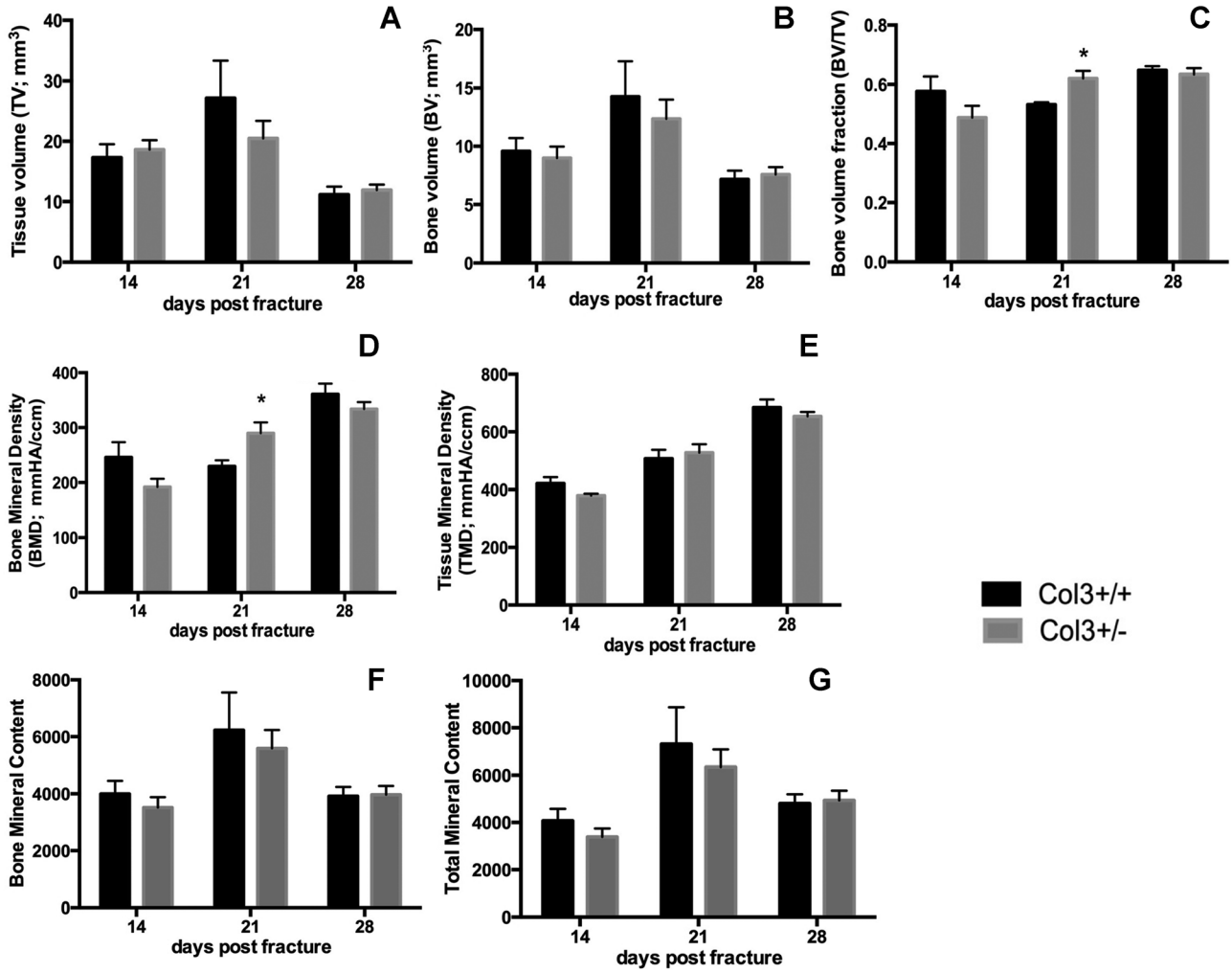

Figure 3. MicroCT analysis of tibial fracture in young adult Col3+/+ and Col3+/− mice. Microcomputed tomography analysis demonstrates significant differences in bone volume fraction and bone mineral density at 21 days post fracture in Col3 wild-type (Col3+/+; black bars) and Col3 haploinsufficient (Col3+/−; gray bars) mice. (A) Quantification of total callus volume (TV), (B) bone volume (BV), (C) bone volume relative to total callus volume (bone volume fraction; BV/TV), (D) bone mineral density (BMD), (E) (callus) mineral density (TMD), (F) bone mineral content (BMC), and (G) tissue (callus) mineral content (TMC) at day 14, 21, and 28 after tibial fracture ($n = 8$–10 per group). $^{*}p < 0.05$.

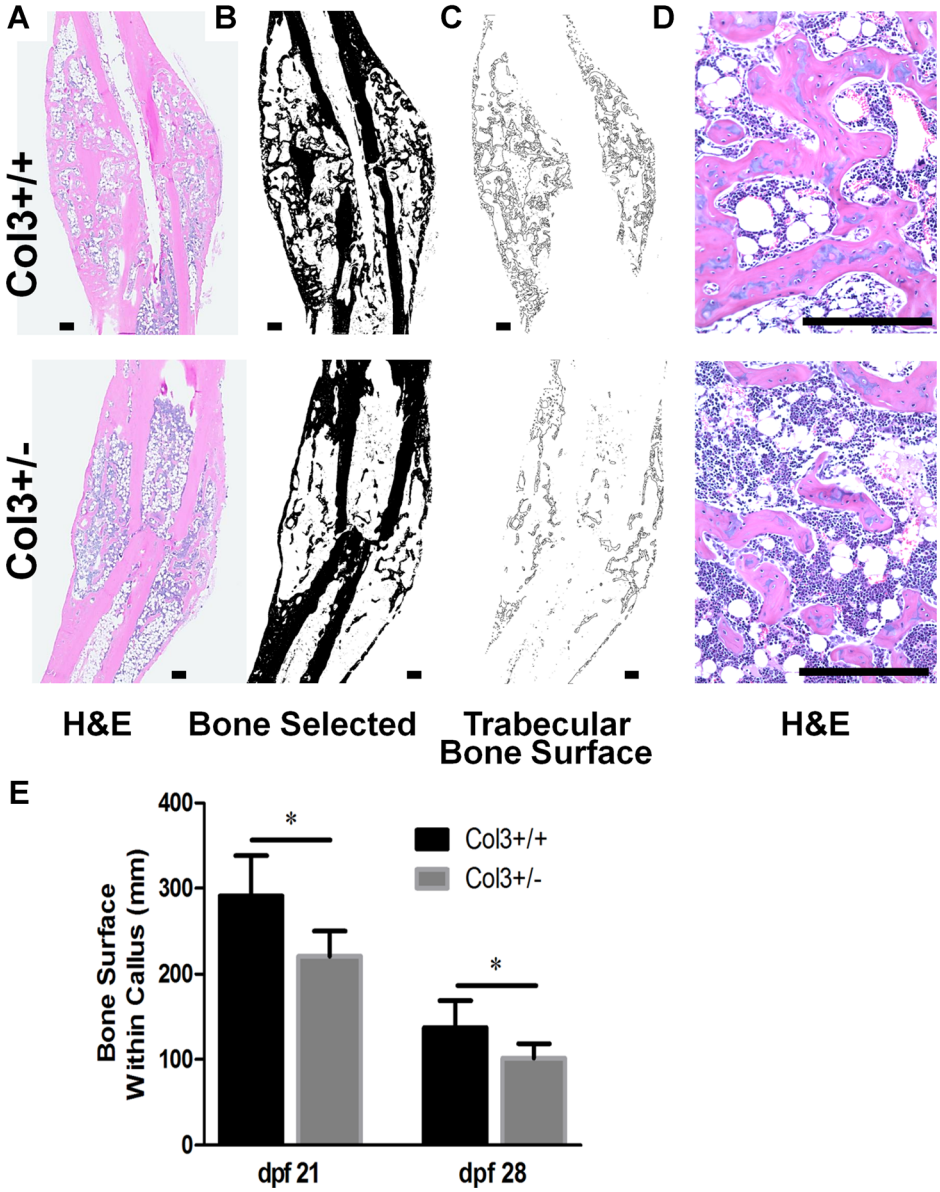

Figure 4. Col3-deficient fractures contain less bone. (A) Representative H&E images of Col3+/+ and +/− fractures 28 dpf. (B) Bone selected and shown in black. (C) The perimeter of the bone within the callus was selected. (D) High magnification images of these fractures show a reduction in the amount of bone in Col3+/− calluses. Scale bar = 250 μm for all images. (E) Quantification of C. Col3+/− fractures have significantly less bone surface within the callus than Col+/+ fractures, $^{*}p < 0.05$.

result of altered cellular proliferation in the fracture callus, we compared PCNA staining in the fracture calluses of Col3+/− and Col3+/+ mice. Undifferentiated mesenchyme of the developing fracture callus showed that proliferation differences (% PCNA-positive staining) were not significantly different between the two genotypes at either day 7 or 14 after fracture (Fig. 5A and B). At day 21, there was a small but insignificant increase in proliferation of cells around the bone perimeter in calluses of Col3+/− mice compared to wild-type mice.

Osteoclast Activity Is Attenuated in the Fracture Callus of Col3+/− Mice Compared to Wild-Type Mice

Because our data suggested alterations in early callus remodeling between the two genotypes, we evaluated osteoclast number using TRAP histochemistry at days 21 and 28 (Fig. 6). Results indicated very low numbers of osteoclasts per bone surface in the Col3+/− mice at day 21, significantly less than that that found in wild-type mice ($p < 0.001$). By day 28, however, there was no significant difference between the wild-type and Col3 deficient mice with respect to osteoclast number, although the density of osteoclasts increased significantly in the fracture callus of Col3 mice from day 21 to 28.

DISCUSSION

Col3 has been proposed to play a role in tissue repair and regeneration due to the early increase in its expression following tissue injury; however, its specific

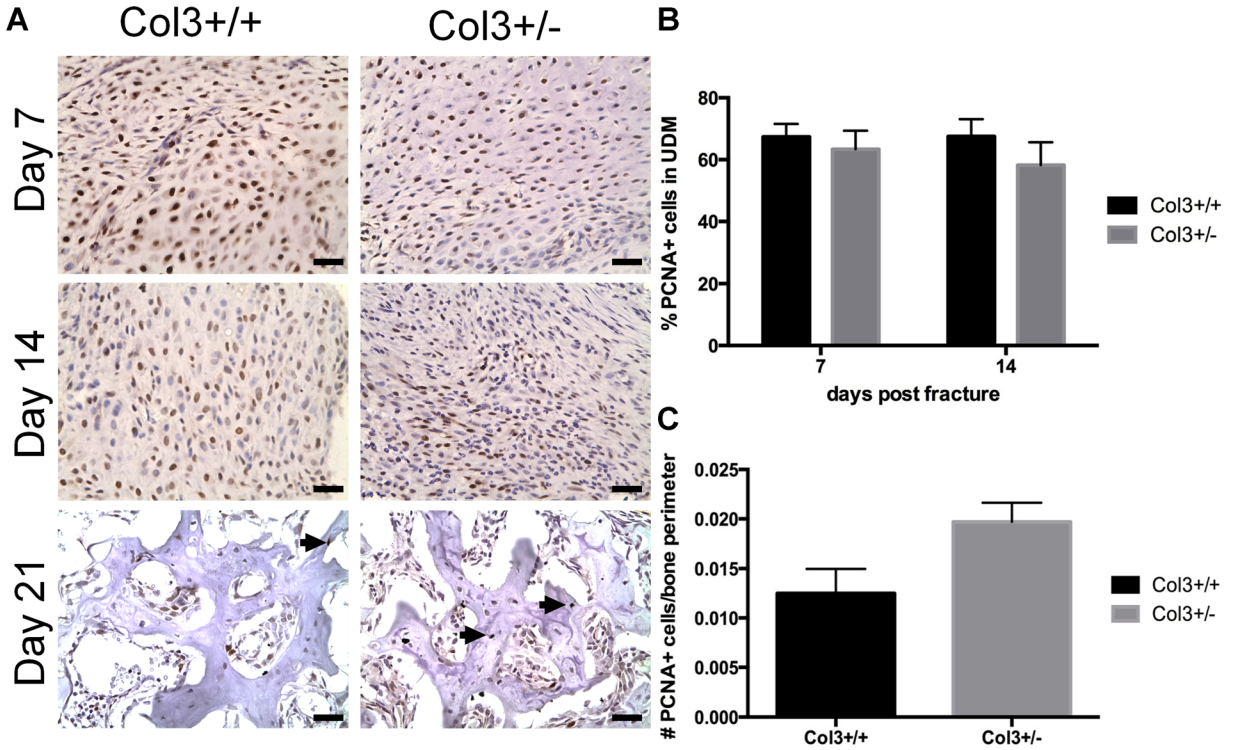

Figure 5. Nuclear proliferation of undifferentiated mesenchyme does not differ between Collagen 3 deficient mice and wild-type mice during fracture healing. (A) Histological sections (40×) of undifferentiated mesenchyme (UDM) around the callus at day 7, 14, and bone (21 days) after fracture show positive PCNA staining (black nuclei). (B) Percent of proliferating cells for both wild-type and Col3+/− mice shows no significant difference in the undifferentiated mesenchyme at either day 7 or day 14 after fracture ($n = 4$–6). (C) Quantification of PCNA positive (proliferating) cells divided by all cells in the bone perimeter for both wild-type and Col3+/− mice shows no significant difference at day 21 after fracture ($n = 4$–6). Scale bars = 25 μm.

role in fracture repair has not been elucidated. Consistent with previous reports citing induction of Col3 expression in the early stages of healing of a variety of tissues,[3–5] our results show that Col3 mRNA levels begin to increase within the first 2 days following long bone fracture and remain significantly elevated over the first 3 weeks. Our data further shows that Col3 is found throughout the undifferentiated mesenchyme, within blood vessels and immature woven bone of the murine fracture callus, similar to its previously described distribution in other species.[6–8,37–39] Col3 is present but diminished, by comparison, within the cartilaginous matrix. Based upon in situ hydridization studies by Bland et al.,[8] it is likely Col3 in the cartilaginous matrix is a remnant from the pre-existing fibrous matrix laid down by mesenchymal progenitors. This expression pattern suggests that Col3 may modulate undifferentiated mesenchymal and osteogenic cell activity and fate during fracture healing, and is in line with its previously defined role in osteoblast differentiation and trabecular bone formation and maintenance. Furthermore, this data also suggests that Col3 is less likely to play a significant role in endochondral ossification,[6] which is further supported by the fact that long bone length is similar between Col3+/+ and Col3+/− mice.[11]

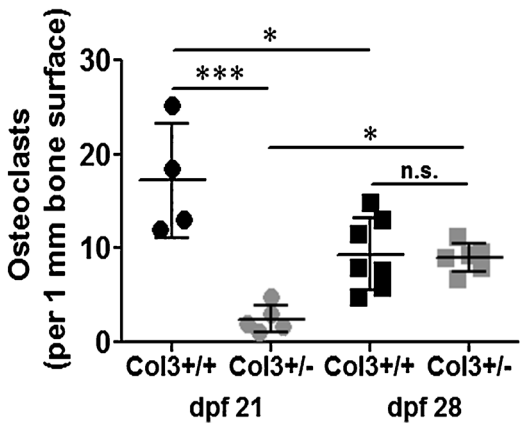

Figure 6. Osteoclast numbers are reduced in Col3+/− compared to Col3+/+ calluses 21 days post fracture. Osteoclasts within the callus 21 and 28 days post fracture (dpf) were identified by TRAP staining. Osteoclast number was normalized to bone surface for quantification. Osteoclast numbers per mm bone surface were significantly reduced in Col3+/− mice dpf 21 when compared to Col3+/+, and osteoclasts decreased between 21 and 28 dpf for Col3+/+ mice, but increased in Col3+/− fractures, $^{*}p < 0.05$ and $^{***}p < 0.001$ via 1-way ANOVA followed by a Tukey post hoc test (n.s., not significant).

As many risk factors associated with poor fracture healing, such as age, smoking, corticosteroid administration, and diabetes, have also been associated with reductions in tissue Col3 expression,[21–27] we examined the hypothesis that fracture repair would be delayed in mice that are haploinsufficient for Col3 compared to wild-type mice. We have previously shown that bone

Col3 mRNA levels of young adult Col3+/− mice are approximately half of that seen in Col3+/+ mice.[11] Our results suggest that a reduction in bone Col3 in young adult mice does not prevent or significantly delay fracture repair, although significant differences do exist in fracture healing between Col3+/− mice and their wild-type littermates. Bone volume (BV) and tissue volume (TV) measured by microCT were not significantly different between genotypes at day 21; however, a disproportionate decrease in TV values in Col3+/− mice likely contributed to a significant increase in bone fraction volume (BV/TV) seen in Col3+/− mice compared to Col3+/+ mice at that time. This was somewhat surprising given the significant increase in BV/TV of uninjured bone in Col3+/+ mice compared to Col3+/− littermates.[11] More consistent with the uninjured bone phenotype is the histologic assessment of bone surface area in the fracture callus, which shows a significant reduction in woven bone within the fracture callus of Col3+/− mice compared to wild-type littermates at days 21 and 28 (Fig. 4). Discrepancy between these two modalities have been noted by others,[40] prompting advocation for complementary analysis using both microCT and histomorphometry. It is possible that the larger trabeculae seen on histology were beneath the single threshold chosen for microCT analysis in this study at the day 21 time point. On the other hand, histological assessment of bone does not set mineral inclusion thresholds for analysis. A smaller but significant reduction in intracallus bone surface was still evident at day 28, suggesting differences between the genotypes were normalizing at that time. Given this normalization of bone surface area and the similarity in bone fraction volume between genotypes, as determined by microCT analysis, it is not surprising that no significant differences were noted in biomechanical properties in torsional testing at that time.

Given the apparent bimodal expression of Col3 in the undifferentiated mesenchyme and later in the immature bone of the fracture callus, we examined the effect of Col3 haploinsufficiency on proliferation of mesenchymal cells. No significant differences were found in proliferation of undifferentiated mesenchyme within the callus between the two genotypes at early time points (day 7 and 14 post fracture), suggesting that Col3 haploinsufficiency does not limit expansion of progenitor cells. We also did not find significant differences in proliferative capacity of cells within newly formed bone of day 21 fractures. We have previously shown that Col3 regulates osteoblastogenesis, and primarily affects trabecular bone development via osteoblast differentiation, with Col3 deficient mice having reduced osteogenesis and less trabecular bone.[11] These findings provide a potential mechanism for the decrease in bone surface area associated with Col3 deficiency (Fig. 4).

In addition, we also examined potential effects of Col3 in modulating osteoclast activity within the fracture callus. Interestingly, TRAP staining revealed a significant reduction in osteoclast activity in the fracture callus of Col3+/− mice at day 21 (Fig. 5). We propose that this transiently decreased osteoclastic activity associated with Col3 deficiency (Fig. 6) is coupled to diminished osteoblast activities at that time[11] and that this decreased osteoclastic response leads to the normalization of early differences in new bone formation between Col3+/− and Col3+/+ mice. However, an alternative hypothesis is that Col3 may directly modulate osteoclast activity. Collectively, our data suggest that Col3 may play its most significant role in the fracture callus through its ability to modulate bone formation and coupled remodeling.

A possible limitation with this study that may explain why a more profound impact of relative Col3 deficiency on fracture repair was not seen was the age of the mice used. The efficiency of healing in the young adult mice used in this study may not have allowed for detection of the full spectrum healing differences in Col3+/− mice. Evidence supporting this possibility include the fact that patients with vascular EDS do not develop clinical symptoms until the 3rd or 4th decade of life.[16] Furthermore, both cutaneous wound healing differences and vascular abnormalities are not evident in Col3+/− mice until at least middle age (>1 year).[10] The exact mechanism for the impact of age on Col3 phenotype during healing is currently under investigation, but may be due to additional modifications to the extracellular matrix (ECM) associated with aging, changes in compensatory factors with age, or may be associated with a further decline in Col3 that accompanies aging[23–25] which results in Col3 falling below a critical level necessary to support efficient repair. Although investigation of the impact of Col3 deficiency in an aged model of fracture repair is beyond the scope of the current investigation, our data suggesting that Col3 modulates the repair process in fracture healing supports future investigation in an aged model to determine a greater role for Col3 in this population of individuals and identify the potential for Col3-biomaterials to accelerate delayed healing in geriatric patients.

ACKNOWLEDGMENTS

The authors wish to thank Dr. Wei-Ju Tseng for assistance with micro-CT analysis and Dr. Michael Dishowitz and Mr. Yanjian Wang for assistance with realtime RT-PCR analysis of collagen expression during fracture repair. S.W. Volk received funding for these studies from the Penn Center for Musculoskeletal Disorders (SLA and SWV) and the National Institutes of Health (K08AR053945 to SWV). K.D. Hankenson is the cofounder of Skelegen, Inc. The remaining authors report no conflicts of interest.

REFERENCES

1. Jahangir AA, Nunley RM, Mehta S, et al. 2008. Bone-graft substitutes in orthopaedic surgery. AAOS Now 2:1–5.
2. Desai BM. 2007. Osteobiologics. Am J Orthop 36:8–11.

3. Merkel JR, DiPaolo BR, Hallock GG, et al. 1988. Type I and type III collagen content of healing wounds in fetal and adult rats. Proc Soc Exp Biol Med 187:493–497.
4. Liu SH, Yang R-S, Al-Shaikh R, et al. 1995. Collagen in tendon, ligament, and bone healing: a current review. Clin Orthop Relat Res 318:265–278.
5. Hurme T, Kalimo H, Sandberg M, et al. 1991. Localization of type I and III collagen and fibronectin production in injured gastrocnemius muscle. Lab Invest 64:76–84.
6. Lane JM, Suda M, von der Mark K, et al. 1986. Immunofluorescent localization of structural collagen types in endochondral fracture repair. J Orthop Res 4:318–329.
7. Ashhurst DE. 1990. Collagen synthesized by healing fractures. Clin Orthop 255:273–283.
8. Bland YS, Critchlow MA, Ashhurst DE. 1999. The expression of the fibrillar collagen genes during fracture healing: heterogeneity of the matrices and differentiation of the osteoprogenitor cells. Histochem J 31:797–809.
9. Liu X, Wu H, Burne M, et al. 1997. Type III collagen is crucial for collagen I fibrillogenesis and for normal cardiovascular development. Proc Natl Acad Sci USA 94:1852–1856.
10. Volk SW, Wang Y, Mauldin EA, et al. 2011. Diminished type III collagen promotes myofibroblast differentiation and increases scar deposition in cutaneous wound healing. Cells Tissues Organs 194:25–37.
11. Volk SW, Shah SR, Cohen AJ, et al. 2014. Type III collagen regulates osteoblastogenesis and the quantity of trabecular bone. Calcif Tiss Int 94:621–631.
12. Hiltunen A, Aro HT, Vuorio E. 1993. Regulation of extracellular matrix genes during fracture healing in mice. Clin Orthop Rel Res 297:23–27.
13. Maehata Y, Takamizawa S, Ozawa S, et al. 2007. Type III collagen is essential for growth acceleration of human osteoblastic cells by ascorbic acid 2-phosphate, a long-acting vitamin C derivative. Matrix Biol 26:371–381.
14. Chen XD, Dusevich V, Feng JQ, et al. 2007. Extracellular matrix made by bone marrow cells facilitates expansion of marrow-derived mesenchymal progenitor cells and prevents their differentiation into osteoblasts. J Bone Miner Res 22:1943–1956.
15. Kanzawa SS, Endo H, Shioya N. 1993. Improved in vitro angiogenesis model by collagen density reduction and use of type III collagen. Ann Plast Surg 30:244–251.
16. Oderich GS, Panneton JM, Bower TC, et al. 2005. The spectrum, management and clinical outcome of Ehlers–Danlos syndrome type IV: a 30-year experience. J Vasc Surg 42:98–106.
17. Dolan AL, Arden NK, Grahame R, et al. 1998. Assessment of Ehlers Danlos syndrome by ultrasound and densitometry. Ann Rheum Dis 57:630–633.
18. Yen J-L, Lin S-P, Chen M-R, et al. 2006. Clinical features of Ehlers–Danlos syndrome. J Formosan Med Assoc 105:475–480.
19. De Coster PJ, Martens LC, De Paepe A. 2005. Oral health in prevalent types of Ehlers–Danlos syndromes. J Oral Pathol Med 34:298–307.
20. Stanitski DF, Nadjarian R, Stanitski CL, et al. 2000. Orthopaedic manifestations of Ehlers–Danlos syndrome. Clin Orthop Rel Res 376:213–221.
21. Oishi Y, Fu ZW, Ohnuki Y, et al. 2002. Molecular basis of the alteration in skin collagen metabolism in response to in vivo dexamethasone treatment: effects on the synthesis of collagen type I and III, collagenase, and tissue inhibitors of metalloproteinases. Br J Dermatol 147:859–868.
22. Tang M, Zhong M, Shang Y, et al. 2008. Differential regulation of collagen types I and III expression in cardiac fibroblasts by AGEs through TRB3/MAPK signaling pathway. Cell Mol Life Sci 65:2924–2932.
23. Takeda K, Gosiewska A, Peterkofsky B. 1992. Similar, but not identical, modulation of expression of extracellular matrix components during in vitro and in vivo aging of human skin fibroblasts. J Cell Phys 153:450–459.
24. Varani J, Dame MK, Rittie L, et al. 2006. Decreased collagen production in chronologically aged skin: roles of age-dependent alteration in fibroblast function and defective mechanical stimulation. Am J Pathol 168:1861–1868.
25. Mays PK, Bishop JE, Laurent GJ. 1988. Age-related changes in the proportion of types I and III collagen. Mech Ageing Dev 45:203–212.
26. Benatti BB, Silverio KG, Casati MZ, et al. 2008. Influence of aging on biological properties of periodontal ligament cells. Connect Tissue Res 49:401–408.
27. Knuutinen A, Kokkonen N, Risteli J, et al. 2002. Smoking affects collagen synthesis and extracellular matrix turnover in human skin. Br J Dermatol 146:588–594.
28. Stevenson K, Kucich U, Whitbeck C, et al. 2006. Functional changes in bladder tissue from type III collagen-deficient mice. Mol Cell Biochem 283:107–114.
29. Cooper TK, Zhong Q, Krawczyk M, et al. 2010. The haploinsufficient Col3a1 mouse as a model for vascular Ehlers–Danlos syndrome. Vet Pathol 47:1028–1039.
30. Miedel E, Dishowitz MI, Myers MH, et al. 2013. Disruption of thrombospondin-2 accelerates ischemic fracture healing. J Orthop Res 31:935–943.
31. Dishowitz MI, Terkhorn SP, Bostic SA, et al. 2012. Notch signaling components are upregulated during both endochondral and intramembraneous bone regeneration. J Orthop Res 30:296–303.
32. Taylor DK, Meganck JA, Terkhorn S, et al. 2009. Thrombospondin-2 influences the proportion of cartilage and bone during fracture healing. J Bone Miner Res 24:1043–1054.
33. Wakamatsu K, Ghazizadeh M, Ishizaki M, et al. 1997. Optimizing collagen antigen unmasking in paraffin-embedded tissues. Histochem J 29:65–72.
34. Meganck JA, Begun DL, McElderry JD, et al. 2013. Fracture healing with alendronate treatment in the Brtl/+ mouse model of osteogenesis imperfecta. Bone 56:204–212.
35. Broz JJ, Simske SJ, Greenberg AR, et al. 1993. Effects of rehydration state on the flexural properties of whole mouse long bones. J Biomech Eng 115:447–449.
36. Kon T, Cho T-J, Aizawa T, et al. 2001. Expression of osteoprotegerin, receptor activator of NF-κB ligand (osteoprotegerin ligand) and related proinflammatory cytokines during fracture healing. J Bone Miner Res 16:1004–1014.
37. Keene DR, Sakai LY, Burgeson RE. 1991. Human bone contains type III collagen, type VI collagen and fibrillin. J Histochem Cytochem 38:59–69.
38. Ford JL, Robinson DE, Scammell BE. 2003. The fate of soft callus chondrocytes during long bone fracture repair. J Orthop Res 21:54–61.
39. Lawton DM, Andrew JG, Marsh DR, et al. 1997. Mature osteoblasts in human non-union fractures express collagen type III. Mol Pathol 50:194–197.
40. Yeo A, Cheok C, Teoh SH, et al. 2012. Lateral ridge augmentation using a PCL–TCP scaffold in a clinically relevant but challenging micropig model. Clin Oral Implants Res 23:1322–1332.

SUPPORTING INFORMATION

Additional Supporting Information may be found in the online version of this article at the publisher's web-site.